

The adsorption of chlorofluoromethane on pristine and Ge-doped silicon carbide nanotube: a PBC-DFT, NBO, and QTAIM study

Mohsen Doust Mohammadi , Idris H. Salih & Hewa Y. Abdullah

To cite this article: Mohsen Doust Mohammadi , Idris H. Salih & Hewa Y. Abdullah (2020): The adsorption of chlorofluoromethane on pristine and Ge-doped silicon carbide nanotube: a PBC-DFT, NBO, and QTAIM study, Molecular Simulation, DOI: [10.1080/08927022.2020.1834103](https://doi.org/10.1080/08927022.2020.1834103)

To link to this article: <https://doi.org/10.1080/08927022.2020.1834103>



Published online: 19 Oct 2020.



Submit your article to this journal [↗](#)



Article views: 4



View related articles [↗](#)



View Crossmark data [↗](#)



The adsorption of chlorofluoromethane on pristine and Ge-doped silicon carbide nanotube: a PBC-DFT, NBO, and QTAIM study

Mohsen Doust Mohammadi^a, Idris H. Salih^b and Hewa Y. Abdullah^b

^aSchool of Chemistry, College of Science, University of Tehran, Tehran, Iran; ^bPhysics Education Department, Faculty of Education, Tishk International University, Erbil, Iraq

ABSTRACT

The feasibility of detecting the chlorofluoromethane (CFM) onto the outer surface of pristine silicon carbide nanotube (SiCNT), as well as its germanium doped structures (SiCGeNT), was carefully evaluated. Density functional theory level of study using the PBE0 functional together with a 6-311G (d) basis set has been used. Subsequently, the B3LYP, CAM-B3LYP, ω B97XD, and M06-2X functionals with a 6-311G(d) basis set were also employed to consider the single point energies. Natural bond orbital (NBO) and quantum theory of atoms in molecules (QTAIM) were implemented by using the PBE0/6-311G(d) method. The total density of states (TDOSs), Wiberg bond index (WBI), natural charge, natural electron configuration, donor–acceptor natural bond orbital interactions, and the second-order perturbation energies are performed to explore the nature of the intermolecular interactions. All results denote that by adsorbing of the gas molecule onto the surface of the considered nanostructures, the intermolecular interactions are of the type of strong physical adsorption. It was revealed that the sensitivity of the adsorption will be increased when the gas molecule interacts with decorated nanotubes and decrease the HOMO-LUMO band gap; therefore, the change of electronic properties can be used to design suitable nanosensors to detect CFM gas.

ARTICLE HISTORY

Received 31 July 2020
Accepted 25 September 2020

KEYWORDS

Chlorofluoromethane; CFM; silicon carbide; Freon 31; natural bond orbital

1. Introduction

The nano materials are structurally divided into carbon and non-carbon materials. carbon nanotube (CNT), which is an allotropes of carbon, were first discovered independently by Iijima et al. [1] and Bethune et al. [2] in 1991 in soot from carbon discharge in a neon-containing medium [3–7]. The CNT, according to its (n,m) type, presents stupendous mechanical [8–10], electromagnetic [11–15], and chemical [16–19] properties and it plays a significant role in various branches of technology. One of the most applicable binary carbide-derived carbons of CNT with extensive properties is silicon carbide nanotube (SiCNT) [20]. There have also been widespread reports on the applications of SiCNT as active material in electrodes [21, 22], gas storage materials [23, 24], and catalysts [25–27].

In the last two decades, theoretical studies in the density functional theory (DFT) framework on nanostructures have attracted the attention of many scientists in the fields of computational chemistry and solid-state physics. The study of silicon carbide nanotube is no exception, and many theoretical studies on this nanostructure have led to interesting proposals for the manufacture of the industrial devices. Theoretical studies show the molecular stability, structure, and properties of SiCNT [28, 29]. In this regard, Alam et al. proved that the most stable form of SiCNT is the arrangement in which the Si atom surrounded by three carbon atoms [30]. Compared to the CNT, the SiC nanotube shows high thermal stability as well as a larger HOMO-LUMO gap (HLG) [31]. Ahmadi

et al. shows by doping the gallium element to the SiCNT, the semiconductor properties will be improved [32]. Having a wide surface, SiCNT can appear in the role of an adsorbent and be used in the design of relevant tools. Mohammadi et al. have had a precise investigation on the adsorption of noble gases and bromomethane onto the SiCNT [33, 34]. A biotechnology study by Chen et al. introduced (8,0) SiCNT for encapsulation of the glycine molecule [35]. Several toxic gases can be trapped using SiCNT such as CO [36], NO [37], N₂O [38], CO₂ [39]. The widespread use of silicon carbide nanotubes, provide the basis for further study on such structures.

Chlorofluoromethane (CFM), (also is known as Freon 31 or HCFC 31 with chemical formula CH₂ClF), is classified as a category 2 carcinogen from the group of chlorofluorocarbons or dihalomethanes. It is a colourless, odourless, flammable gas with a solid monoclinic crystal structure of space group P21 [40]. Chlorofluoromethane was used as the refrigerant. It is listed in the Montreal Protocol as a substance that degrades the ozone layer [41]. A rotational study has been performed by Caminati et al. [42] to investigate the dimer interactions of CFM molecule and the results confirm that the interactions are non-covalent. According to the dissociation energy of dimer complex of CFM molecule reported in [42] we considered it as an isolated single molecule in this work.

This article discusses the design of such a sensor. This study investigated the interactions of CFM with SiCNT and SiCGeNT. After optimising the structure of silicon carbide nanotubes by Gaussian software, to study the chemical stability and

conductivity, the elements doping process on this nanotube have been studied. Because of the high sensitivity of computation to precisely determine the energy of molecular orbitals to investigate the conductivity and probability of physical and chemical adsorption, different structures need to be optimised using appropriate computational methods. For this purpose, the PBE0 functional and 6-311G(d) basis set was used in this research for computation. The B3LYP, CAM-B3LYP, ω B97XD, and M06-2X functionals with 6-311G (d) basis set were also used to calculate the single point energies. Natural bond orbital and quantum theory of atoms in molecules were studied by using the PBE0 /6-311G (d) method and the results were used to obtain various physical parameters.

2. Computational details

The DFT calculations at Perdew, Burke, and Ernzerhof (PBE0) functional [43] together with 6-311G(d) Pople split-valence triple-zeta basis set with polarisation functions [44] were used for geometry optimisation for all different positions of the CFM/tube complex structures. To determine the stability of the optimised structures, frequency calculations are also performed using the similar level of theory to approve that all the stationary points are in agreement with a minimum point through the potential energy surface. For further investigation, single point energy calculations using different levels of theory were also applied on the most stable relaxed structures, which were obtained from geometry optimisation at the PBE0/6-311G(d) level. The levels of theory used for the single point energy calculations included B3LYP, CAM-B3LYP, M06-2X, ω B97XD together with 6-311G(d) basis set. Natural bond orbital (NBO) and quantum theory of atoms in molecules (QTAIM) were implemented by using the PBE0/6-311G(d) method. All of the calculations including geometry optimisation, single point energy calculations, and NBO analysis were performed by Gaussian 16 package [45]. It should be noted that the NBO calculations were performed using NBO v 3.1 software which is embedded within Gaussian software. In order to perform quantum theory of atoms in molecule (QTAIM) and density of state (DOS) analyses, the Multiwfn program [46–48] was employed.

The adsorption energy (E_{ads}) of the investigated CFM onto the surface of pristine and doped nanotubes can be calculated as follows:

$$E_{\text{ads}} = E_{\text{sheet/CFM}} - (E_{\text{sheet}} + E_{\text{CFM}}) \quad (1)$$

where $E_{\text{tube/CFM}}$ represents the total energy of the complex structure. E_{tube} and E_{CFM} , are the total energy of the pure nanotube and the pure CFM molecule, respectively. It is noteworthy that the absorption energy consists of two parts: the interaction energy (E_{int}) and the deformation energy (E_{def}) that occur in the absorption process. Therefore, the following

equations are used to calculate these shares:

$$E_{\text{ads}} = E_{\text{int}} + E_{\text{def}} \quad (2)$$

$$E_{\text{int}} = E_{\text{sheet/CFM}} - E_{\text{sheet in complex}} - E_{\text{CFM in complex}} \quad (3)$$

$$\begin{aligned} E_{\text{def}} &= E_{\text{def}}^{\text{sheet}} + E_{\text{def}}^{\text{CFM}} \\ &= (E_{\text{sheet in complex}} - E_{\text{pristine sheet}}) \\ &\quad + (E_{\text{CFM in complex}} - E_{\text{isolated CFM}}) \end{aligned} \quad (4)$$

where $E_{\text{sheet in complex}}$ and $E_{\text{CFM in complex}}$ are energies of CFM molecule and nanotube in the optimised complexes, respectively.

3. Result and discussion

3.1. The structural analysis

To optimise the structure of pristine armchair (5,5) single walled silicon carbide nanotubes using periodic boundary conditions, we first consider a unit cell of silicon and carbon atoms ($\text{Si}_{20}\text{C}_{20}$) which is 6.274 Å in length. Unlike the nanosheet, the nanotube is expanded in one direction only. We optimised this cell by 1D periodic boundary condition DFT method with PBE0 functional together with basis set 6-311G (d). After optimisation of the pristine unite cell we substituted Ge with Si atom then the optimisation process has been repeated for doped nanotubes. The quantitative values of bond lengths are shown in Figure 1.

The next step was the optimisation of CFM/nanotube complexes. In this step the CFM molecule was placed on the outer surface of each above-mentioned nanotubes with vertical distance of about 2.1 Å. To find out the optimum distances between nanotube and CFM molecule we used the rigid scan for some cases to estimate the most efficient distance. It should be noted that the level of theory in both optimisation and rigid scan was PBE0/6-311G (d). To better explain the details of the adsorption process, it will be useful to compare Figures 1 and 2.

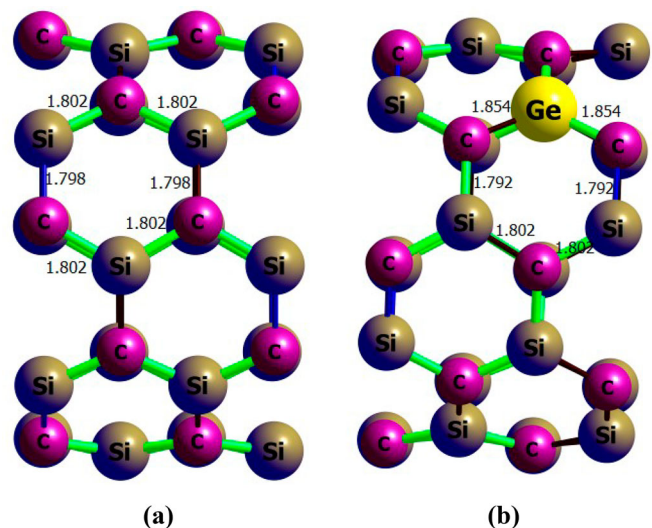


Figure 1. (Colour online) The values of bond length for (a) SiCNT and (b) SiGeNT. The optimisation process has been done using PBE0/6-311G (d) level of theory.

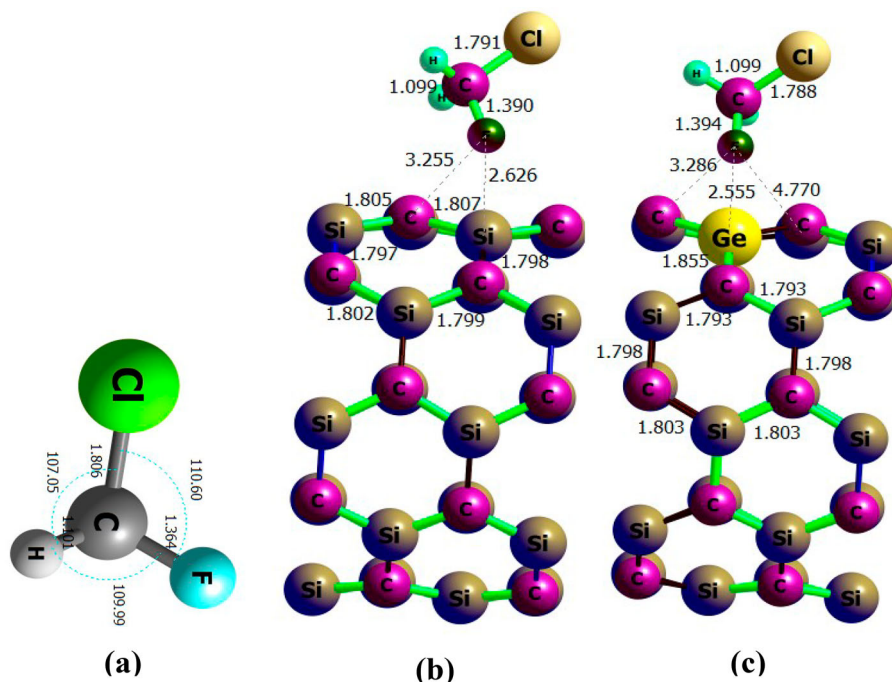


Figure 2. (Colour online) The most stable form of (a) isolated CFM and the adsorbed CFM molecule onto the outer surface of (b) SiCNT and (c) SiCGeNT. All clusters have been optimised using the PBE0 functional and 6-311G (d) basis set.

The silicon carbide nanotube is composed of several symmetric hexagons that have four different adsorption positions for the adsorption of any molecule onto the outer surface of the nanotube as shown in Figure 3: adsorption position on Si atom (T_1); adsorption position on C atom (T_2); and adsorption position on Si–C bond (T_3); adsorption position at hexagonal center (T_4). The logical approach is to put the CFM molecule in each of these positions and measure the amount of adsorption energy (E_{ads}). It is important to note that the CFM molecule has different heads (H, Cl, F), and each of these heads must be placed on the desired position on the nanotube to measure the amount of absorption energy. Our

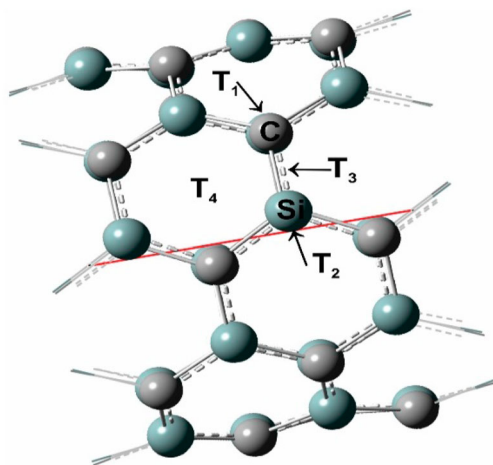


Figure 3. (Colour online) All possible target positions for the adsorption of any arbitrary molecules onto the surface of SiCNT. Top of boron atom (T_1), top of nitrogen atom (T_2), between boron and nitrogen atoms (T_3), and top of the hexagonal ring (T_4).

experience shows that negligible differences exist in the amounts of adsorption energies when we place the CFM in any of the possible adsorption sites. As mentioned in [49], when the differences in the adsorption energies are ‘below the range of chemical interest’, placing the gas in different positions on the nanotubes provides identical results. Nevertheless, we put the CFM molecule from F-head onto the desired positions on the SiC nanotube. The test result showed that there is a negligible difference among the adsorption energies; therefore, the boron atom position was the target position on the SiC nanotube.

Next, we extend the unit cell to five units and terminated with hydrogen atoms (Figure 4), the nanotube length for Si₁₀₀-C₁₀₀H₂₀ increased to 31.804 Å, then single point energy calculations using different functional such as: PBE0, ω B97XD, and M06-2X and 6-311G (d) basis set were done. The calculated values indicate a strong interactions between nanotubes and CFM molecule. Since the PBE0 functional does not account for the long-range scattering contribution, it is expected that in poor interactions, this functional will not give a good estimate of the amount of energy. For this reason, methods have been developed for long-range and dispersion effects. In this work we used PBE0, ω B97XD to consider long range and dispersion effects. The well-known M06-2X functional are used to better comparison. The results show that the energies obtained from the PBE0 and other functionals are consistent with the accuracy of the calculations. On the other hand, as expected, the ω B97XD method shows more energy values than the others, due to the dispersion contribution consideration. Also by doping the Ge element on the SiC nanotube, significant changes in the results are achieved. Table 1 shows that Ge doping increase the absorption energy and enhanced the chemical absorption. Table 2 also shows the bond length and

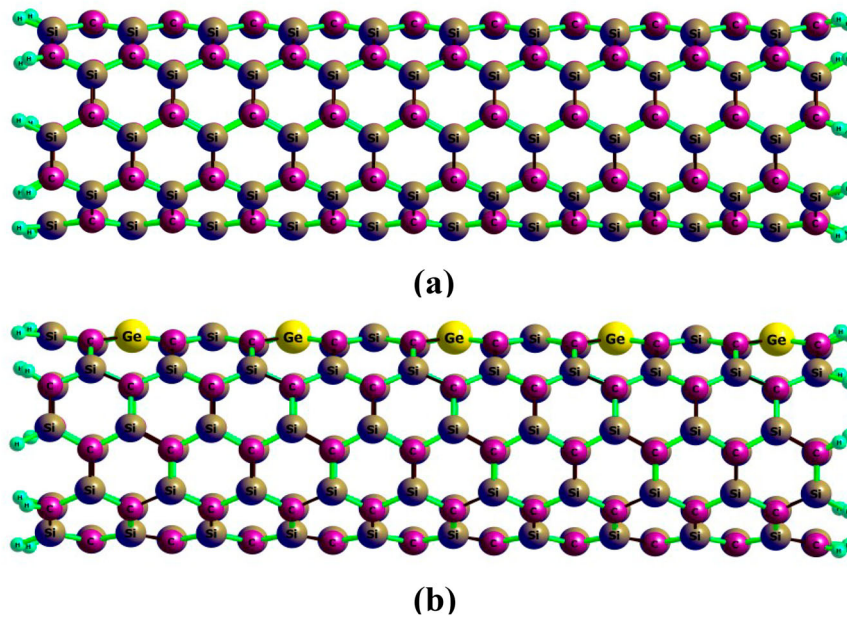


Figure 4. (Colour online) The expanded (a) silicon carbide and (b) Ge-doped silicon carbide nanotubes terminated with hydrogen atoms.

Table 1. The interaction energy (E_b) for SiCNT and SiCGeNT with CFM molecule.

System	PBE0	B3LYP	CAM-B3LYP	M06-2X	ω B97XD
CH ₂ ClF_SiCNT	-1.339	-0.957	-1.400	-1.753	-1.894
CH ₂ ClF_SiCGeNT	-2.748	-2.306	-2.856	-3.507	-3.465

All values are in (eV).

the nearest intermolecular distances (re (Å)) between CFM molecule and SiCNT and SiCGeNT.

3.2. Energetics properties

The chemical electron potential (μ) describes the tendency of electrons to escape from a particular species at the ground state. This quantity is equal to the absolute negative electronegativity obtained from the definition provided by Mulliken, as follows:

$$\mu = -\chi \quad (5)$$

Parr and his colleagues [50] used the DFT to show that at a constant external potential, the potential energy of an electron is related to the first derivative of energy relative to the number of electrons, as follows:

$$\mu = \left(\frac{\partial E}{\partial N} \right)_{v(r)} = -\frac{1}{2}(IP + EA) \quad (6)$$

where IP and EA are the ionisation affinity and electron

affinity, respectively [51]. Based on the Koopman approximation (see the Hartree–Fock theory) and Janak's approximation [52] (in the DFT theory), the ionisation and electron affinity potentials are equal to the negative value of the highest occupied molecular orbital (HOMO) energy ($\varepsilon_{HOMO} = -IP$) and negative value of the lowest unoccupied molecular orbital (LUMO) ($\varepsilon_{LUMO} = -EA$). Therefore, the chemical potential in Janak's approximation is defined as

$$\mu = \left(\frac{\partial E}{\partial N} \right)_{v(r)} \cong \frac{(\varepsilon_{LUMO} + \varepsilon_{HOMO})}{2} \quad (7)$$

where ε_{HOMO} and ε_{LUMO} are the energies of the HOMO and the LUMO, respectively. N is the number of electrons, E is the total electronic energy of the system, and $v(r)$ is the external potential.

Comparison of the variation in electron chemical potentials to that in the number of electrons at a constant external potential is called chemical hardness, which is expressed as

$$\eta = \left(\frac{\partial \mu}{\partial N} \right) = \frac{1}{2} \left(\frac{\partial^2 E}{\partial N^2} \right) \quad (8)$$

Parr et al [53] used the electron energy curve as well as the finite difference approximation to express hardness as follows:

$$\eta = \frac{1}{2}(IP - EA) \quad (9)$$

Table 2. The bond lengths and the nearest intermolecular distances (re (Å)) between CFM molecule and SiCNT and SiCGeNT.

Systems	F-Ge	F-C	F-Si	C-Ge	Si-C	C-H	C-Cl	C-F
CH ₂ ClF	-	-	-	-	-	1.101	1.806	1.364
SiCNT	-	-	-	-	1.800	-	-	-
SiCGeNT	-	-	-	1.854	1.792	-	-	-
CH ₂ ClF/SiCNT	-	3.255	2.626	-	1.807	1.099	1.791	1.390
CH ₂ ClF/SiCGeNT	2.555	3.286	4.770	1.855	1.793	1.099	1.788	1.394

All calculations were performed using PBC-DFT PBE0/6-311G(d) level of theory.

Moreover, using Janak and Koopman's approximations, the hardness equation is transformed as follows:

$$\Delta E_{\min} = -\frac{\mu^2}{2\eta} \quad (10)$$

Chemical hardness is the energy gap between the HOMO and the LUMO. Therefore, molecules with high energies are considered as hard molecules, while those with low energies are called soft molecules. Since the softness of a molecule is the opposite of its hardness, the equation for molecule softness is denoted as follows [54]:

$$S = \frac{1}{\eta} \quad (11)$$

Inspired by Maynard's work, Parr et al [55] introduced electrophilicity as the steady-state energy in which an atom or a molecule at ground state gains by receiving additional electron charges from the environment. The energy changes that lead to such a charge transfer are expressed as follows:

$$\Delta E = \mu\Delta N + \frac{1}{2}\eta(\Delta N)^2 \quad (12)$$

When the system receives electron charges from the environment sufficient to equate its potential to that of the environment, the system is saturated with electrons and can be expressed as follows:

$$\frac{d\Delta E}{d\Delta N} = 0 \quad (13)$$

The electron load received from the environment is maximised, and the total energy of the system is eventually minimised. Thus,

$$\Delta N_{\max} = -\frac{\mu}{\eta} \quad (14)$$

$$\Delta E_{\min} = -\frac{\mu^2}{2\eta} \quad (15)$$

Since $\eta > 0$, $\Delta E < 0$ always, and the charge transfer is energetically desirable. Accordingly, Parr et al. proposed the following equation to denote the electrophilicity of electrophilic species.

$$\omega = \frac{\mu^2}{2\eta} \quad (16)$$

In fact, the electrophilicity index is the capacity of a species to accept an arbitrary number of electrons from the environment. In this regard, Nourizadeh and Maihmi [56] used electrophilicity in the Diels–Alder reaction and stated that ‘atoms appear to be arranged in a natural tendency to reach the lowest electrophilicity.’ This expression is called the minimum electrophilicity principle (MEP).

The values of maximum occupied molecular orbital (HOMO) and lowest occupied atomic orbital (LUMO) and their differences (HLG), chemical potential (μ), chemical hardness (η), and electrophilicity (ω) are reported in Table 3. From the results of this table, it can be seen that by adsorption of CFM molecule onto the outer surface of nanotubes the

Table 3. Values of HOMO energy (ϵ_H), LUMO energy (ϵ_L), HOMO and LUMO energy gap (HLG), chemical potential (μ), chemical hardness (η), and electrophilicity (ω).

System	ϵ_H	ϵ_L	HLG	μ	η	ω
SiCNT	-4.818	-2.723	2.095	-3.770	1.048	7.447
SiCGeNT	-4.805	-2.735	2.070	-3.770	1.035	7.355
CH ₂ ClF/SiCNT	-4.696	-2.668	2.029	-3.682	1.014	6.876
CH ₂ ClF/SiCGeNT	-4.662	-2.666	1.996	-3.664	0.998	6.697

All values are in (eV) and were obtained from completed nanotube PBE0/6-311G (d) level of theory.

distance between HOMO and LUMO levels is reduced relative to the pure nanotube, which is caused by the molecular energy absorption matched from this position. By doping the elements Al and Ga, it is observed that HLG changed. The decrease in HLG results in an increase in the electrical conductivity and thus an increase in the metal property of all the nanotubes compared to pure SiCNT. It is also noteworthy that the observed changes in HLG after doped Ge is mainly due to lower LUMO energy levels. In order to study these changes in the electron structure of the studied cases more closely, the density of state spectra (DOS) will be analyzed in the next section. For a more detailed study of the electron structure changes, the density of state spectra (DOS) are extracted and illustrated in Figure 5.

From the DOS spectra, it is clear that DOS spectra for all absorption are in agreement with the values of the energy parameters reported in Table 3. The lowest amount of adsorption energy is related to the pristine nanotube and the highest amount of adsorption energy is for the adsorption of CFM onto the Ge-doped SiC nanotube, the most changes are also observed in the DOS spectrum relative to this nanotube. In other words, the electron structure changes show a direct relationship with the absorption energies. Given the amount of absorption energy, high amount of binding energy, and the structure of DOS spectra obtained in all of these cases, it can be claimed that the adsorption of CFM molecule onto SiC and SiCGe nanotubes is a strong physical adsorption type.

3.3. NBO and QTAIM analyses

The natural bond orbital (NBO) analysis has been developed based on many-electron molecular wavefunction in terms of localised electron-pair bonding units and uses first-order reduced density matrix of the wavefunction [57, 58]. In the NBO approach, a given wavefunction should be transformed into a localised form in which NBOs are considered as local block eigenfunctions of the density matrix. NBO analysis is applicable in both closed-shell and open-shell systems which are calculated from atom-centered basis functions [59]. The mechanism of the energetic analysis of NBO interactions is based on the one-electron effective energy operator (Fock or Kohn–Sham matrix) that arise from the host electronic structure system (ESS). Second-order perturbation theory is one of the highest uses methods for estimating energy effects. For the case of HF or DFT methods, the interactions between NBOs are considered to analyze the wavefunction energetically. With the explanation that the Kohn–Sham matrix elements are implemented in the DFT platform [60–70].

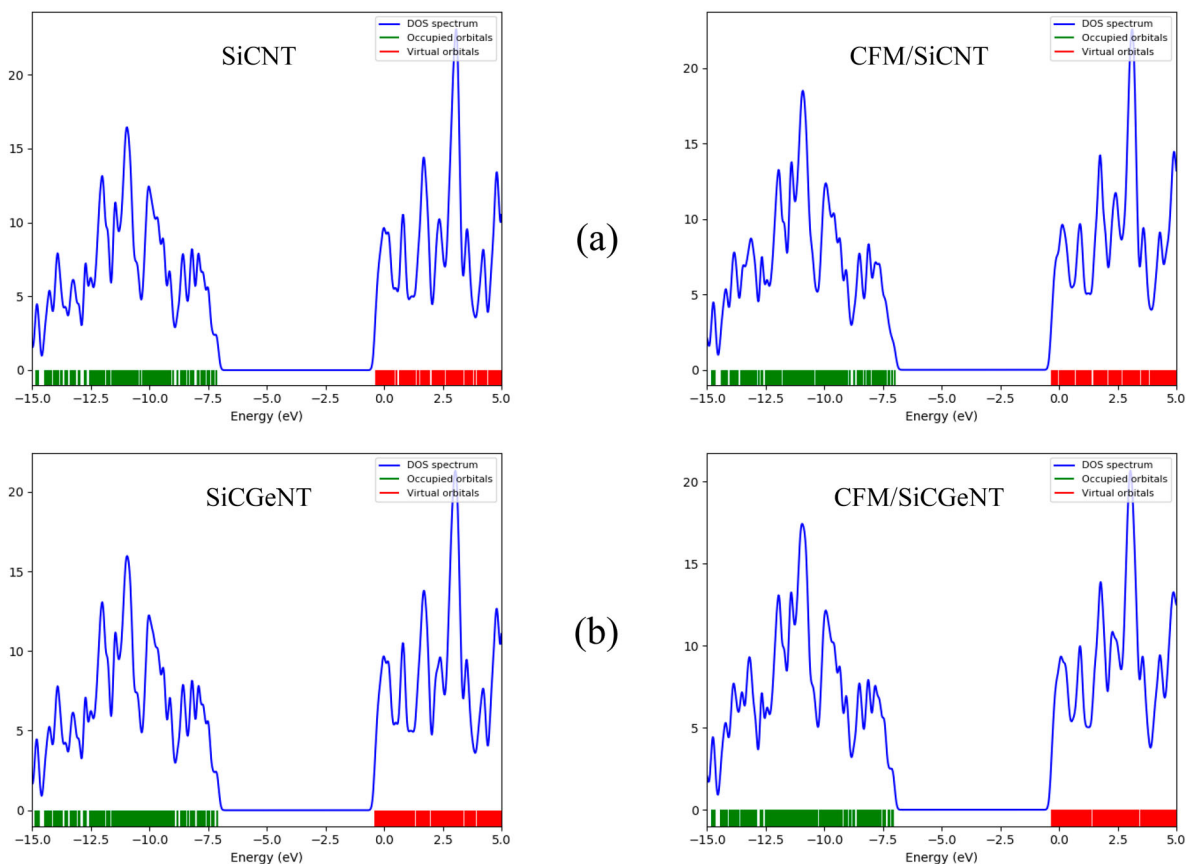


Figure 5. (Colour online) The density of state (DOS) diagrams for the adsorption of CFM molecule onto the surface of the (a) pristine and (b) Ge-doped silicon carbide nanotubes. The data were obtained from completed nanotube and PBE/PBE/6-311G (d) level of theory. The left side diagrams are isolated nanotubes and the right side diagrams are CFM/nanotube clusters.

We used the PBE/PBE/6-311 g(d) level of theory to perform the NBO calculations. The concept of bonded orbitals can be used to understand the distribution of electrons in atomic and molecular orbitals. Atomic charges and molecular bonds can be used to obtain these orbitals. In this method, an electron density matrix is used to both define the shapes of the atomic orbitals in the molecular environment and obtain molecular bonds (electron density between atoms). NBO is defined as the following equation for σ bonding between atoms A and B.

$$\sigma_{AB} = C_A h_A + C_B h_B \quad (17)$$

where h_A and h_B are natural hybrids on the A and B atoms. In the covalent limit, $C_A = C_B$, and at the ionic limit, $C_A \gg C_B$ (if the electronegativity of A is greater than B). Each bonding NBO must be paired with a corresponding anti-bonding NBO.

$$\sigma_{AB}^* = C_A h_A - C_B h_B \quad (18)$$

Bonding orbital analysis is used to evaluate the effects of non-stationary effects, such as anomeric effect, rotation barrier, hydrogen bonding, and so on. In NBO analysis, molecular energy is divided into two parts: total energy (for non-stationary enters) and Lewis molecule energy (where super-conjugation does not occur, and the electrons are strongly bound in single bonds and pairs). The occupied NBOs describe the covalent effects in the molecule, while the non-occupied NBOs are used to describe non-covalent effects. The most

important non-occupied NBOs are anti-bond orbitals [58, 67, 69].

Various types of bond order analyses are developed to take into account the bond property such as Mulliken bond order analysis [71], Mayer bond order analysis [72, 73], Multi-center bond order analysis [74, 75], Wiberg bond order analysis [76], Fuzzy bond order [77, 78] and so on. Due to the different assumptions, caution should be exercised when using the above-mentioned methods and the term 'Caveat emptor' in this case is a practical example to describe such a situation. Basis set containing diffuse functions as case in point, leads to unreliable result for Mulliken or Mayer analyses [46]. According to the literature [79], the Wiberg bond order, in comparison to the Mayer method, has much less sensitivity to the basis set. The Wiberg bond index (WBI) is the sum of squares of off-diagonal density matrix elements between atoms and is denoted as follows:

$$WBI = \sum_k p_{jk}^2 = 2p_{jj} - p_{jk}^2 \quad (19)$$

where P_{jk} represents the density matrix elements (i.e. the contribution of interactions between basis functions j and k) and P_{jj} is the charge density in the atomic orbital. In the WBI, there is no difference between net bonding or antibonding type of elements of the density matrix.

NBO analysis was used to calculate the bond order using the Wiberg method [76] for a more detailed examination of the

types of interactions. After studying the adsorption energy of the complexes, we examine the bond length and bond order of the gases and the nanotubes before and after the adsorption. The Wiberg bond order for these clusters are reported in Table 4. According to this table, that the bond of the halogen atoms in CFM molecules oriented to the Si in SiCNT and Ge in SiC-GeNT. The results of the WBI analysis agree with the adsorption energies reported in Table 1. They reveal that these nanotubes show a strong interaction with the gas molecules and can be considered a suitable sensor for such gases.

One of the results of the natural population analysis obtained from NBO calculation is a natural electron configuration which shows the effective valence electron configuration for any atoms in the studied structure. The results of the NBO calculations shed light on the natural electron configuration and partial natural charge, which are useful in the study of the character of the bond between the CFM and the nanotubes. The NBO approach was implemented for all atoms in the pristine and cluster systems to reveal the quantities listed in Table 5. Charge transfer quantity between CFM molecule and nanotubes can also be a criteria to study the interaction of nanotube and CFM, such that the stronger the interaction the more the charge transfer between CFM and the nanotube. Table 5 shows that there is a significant charge transfer between two species during adsorption process would be happened.

In addition, by implementing the natural electron configuration the type of the interaction between nanotubes and CFM molecule will be described. From Table 5, it can be obvious that valance configuration of isolated CFM molecule and nanotubes as well as valance configuration of nanotube/CFM clusters have been increased. Therefore; the interaction of CFM with all nanotubes can be classified as a strong physical adsorption process.

The second-order perturbative estimate of donor-acceptor interactions in the NBO basis. NBO analysis expresses the complex quantum-mechanical wavefunction into a more palpable Lewis-dot-like formalism. Lewis-type NBOs are called filled or 'donor' orbitals (σ) and Non-Lewis-type NBOs are called vacant or 'acceptor' orbitals (σ^*). For each donor NBO (i) and acceptor NBO (j), the stabilisation energy $E(2)$ is calculated as follow [64]:

$$E(2) = \Delta E_{ij}^2 = -q_i \frac{(F_{ij})^2}{(\epsilon_j - \epsilon_i)} \quad (20)$$

where ϵ_i , ϵ_j are diagonal elements which show the orbital energies, q_i denotes the donor orbital occupancy ($q = 2$ for closed-shell systems and $q = 1$ for open-shell systems), and the off-diagonal NBO Fock matrix element is demonstrated by $F(i, j)$, and ΔE_{ij}^2 is the stabilisation energy.

The results of electron donor-acceptor electron configuration of pristine SiCNT and Ge-doped SiCNT are reported in Table 6. It is noteworthy that in this table the most important interactions in terms of the electron transfer stability energy are reported. The existence of such interactions with the remarkable stability energies in this table shows that the doped atom has been incorporated into the nanotube structure by the chemical interaction and the stability structure has been achieved. In other words, the inserted atom behaves as a doping atom. The data in Table 6 show that the most important interaction for the pristine nanotube related to electron transfer from the BD (Si-C) bond as the electron donor to the BD* (C-F) as the receptor. This is in agreement with the results of the absorption energy as well as with the other results which have examined. In the study of the doped complexe, it is observed that in the Ge electron pair is a donor (Lewis base) and the F-bonded electron pair is the group of the electron acceptor molecule (Lewis acid). The highest electron-acceptor stabilisation energy in all cases is due to the same interaction, which indicates a strong adsorption of the molecule onto the SiCGe nanotube compared to the pristine NT.

3.4. QTAIM analysis

QTAIM is a powerful tool for topology analysis containing the type and structure of bonds and intermolecular interactions.

Table 5. Natural electron configurations and natural charges (esu) for the isolated CFM, pristine and Ge-doped SiCNT nanotubes and their complex structures.

Systems	Atom	Natural charge	Natural electron configuration
SiCNT	Si	1.87	[core]3S(0.70)3p(1.41)3d(0.03)
	C	-1.87	[core]2S(1.35)2p(4.51)
SiCGeNT	Si	1.87	[core]3S(0.70)3p(1.41)3d(0.03)
	C	-1.87	[core]2S(1.35)2p(4.51)
CH ₂ ClF/SiCNT	Ge	1.72	[core]4S(0.86)4p(1.42)4d(0.01)
	Si	1.87	[core]3S(0.69)3p(1.41)3d(0.03)
	C	-1.87	[core]2S(1.35)2p(4.52)
	H	0.24	1S(0.75)
	Cl	-0.06	[core]3S(1.87)3p(5.17)3d(0.01)4p(0.01)
	F	-0.31	[core]2S(1.84)2p(5.46)
	C	-0.05	[core]2S(1.14)2p(2.89)3p(0.01)3d(0.01)
CH ₂ ClF/SiCGeNT	Si	1.87	[core]3S(0.69)3p(1.41)3d(0.03)
	C	-1.87	[core]2S(1.35)2p(4.52)
	Ge	1.75	[core]4S(0.86)4p(1.38)4d(0.01)5p(0.01)
	H	0.24	1S(0.75)
	Cl	-0.05	[core]3S(1.87)3p(5.16)3d(0.01)4p(0.01)
	F	-0.31	[core]2S(1.85)2p(5.46)
	C	-0.06	[core]2S(1.14)2p(2.89)3p(0.01)3d(0.01)

All values calculated by the PBE0/6-311G(d) level of theory.

Table 4. The Wiberg bond index (WBI), obtained for atomic bonds and intermolecular interactions between CFM molecule and SiCNT and SiCGeNT.

Systems	F-Ge	F-C	F-Si	C-Ge	Si-C	C-H	C-Cl	C-F
CH ₂ ClF	-	-	-	-	-	0.909	1.014	0.905
SiCNT	-	-	-	-	0.968	-	-	-
SiCGeNT	-	-	-	0.936	0.974	-	-	-
CH ₂ ClF/SiCNT	-	0.009	0.083	-	0.973	0.906	1.039	0.852
CH ₂ ClF/SiCGeNT	0.093	0.010	0.002	0.895	0.984	0.904	1.044	0.844

All calculations were performed using PBE0/6-311G(d) level of theory.

Table 6. The donor-acceptor NBO interactions and second order perturbation energies ($E(2)$) for the CFM clusters with SiCNT and SiCGeNT.

Systems	Donor NBO (i)	Acceptor NBO (j)	E2 (kcal/mol)
CH ₂ ClF/SiCNT	BD (Si-C)	BD*(C-H)	0.88
	BD (Si-C)	BD*(C-Cl)	0.06
	BD (Si-C)	BD*(C-F)	0.22
	BD (Si-C)	RY*(F)	0.07
	BD (Si-C)	RY*(H)	0.1
CH ₂ ClF/SiCGeNT	BD (Si-C)	BD*(C-H)	0.4
	BD (Si-C)	BD*(C-Cl)	0.15
	BD (Ge-C)	BD*(C-F)	0.39
	BD (Ge-C)	RY*(F)	0.08
	BD (Ge-C)	RY*(H)	0.11
	BD (Ge-C)	RY*(H)	0.09

All values obtained from completed nanotubes at the PBE0/6-311G (d) level of theory.

QTAIM method proposed by Bader et al [80–85]. According to this theory, the critical point of the electron density, which can be a minimum point, a maximum point, or a saddle point, can fall into one of the following four categories: (1) *Atomic critical point* (ACP), which denotes the geometrical position of an atom or nucleus (other than hydrogen), and geometrically represents a local maximum point of electron density in all three directions of space; (2) *bond critical point* (BCP), which indicates a critical point related to a bond or physical or chemical interaction (in reality, this point represents a saddle point with two directions of maximum electron density and one direction of minimum electron density); (3) *ring critical point* (RCP) [86, 87], which denotes a ring or set of atoms forming a ring (geometrically, it is a saddle point with the minimum electron density in one direction and in the other two directions); and (4) *cage critical point* (CCP), which is observed when multiple rings form a cage (geometrically, this point is a local minimum point in all three directions of space). Poincaré-Hopf relationship should be satisfied to verify if all CPs may have been found as follows [88, 89]:

$$n_{(ACP)} - n_{(BCP)} + n_{(RCP)} - n_{(CCP)} = 1 \quad (21)$$

The eigenvalues of Hessian matrix, λ_1 and λ_2 , are negative and $|\lambda_1| < |\lambda_2|$ for the BCP. λ_1 and λ_2 are perpendicular to the bonding path, and λ_3 is a positive value along the bonding path. For the QTAIM analysis, is it necessary to know the

electron density $\rho(r)$ and Laplacian electron density $\nabla^2 \rho(r)$. The $\rho(r)$ and $\nabla^2 \rho(r)$ play an important role in the segmentation and identification of different types of chemical interactions. A BCP with negative values of $\nabla^2 \rho(r)$ and large values of $\rho(r)$ (of orders exceeding 10–1 a.u.) is defined as a shared (covalent) intermolecular interaction. Also, when $\nabla^2 \rho(r)$ is positive, the interactions can be classified as of the non-substrate close-shell type (which include ionic and van der Waals interactions) [90]. The elliptical bond (ϵ) [91] and the virial theorem [92] are two other important factors in the classification of bonds. An elliptical bond represents the electron density preferentially accumulated on a plate containing the bond and is defined as follows:

$$\epsilon = \frac{\lambda_1}{\lambda_2} - 1 \quad \text{where } |\lambda_1| > |\lambda_2| \quad (22)$$

Large values of ϵ indicate an unstable structure and vice versa. Also, based on the virial theorem, the following relationship exists between the electron kinetic energy density $G(r)$ [93], the electron potential energy density $V(r)$ [94], and $\nabla^2 \rho(r)$:

$$\frac{1}{4} \nabla^2 \rho(r) = 2G(r) + V(r) \quad (23)$$

The balance between $G(r)$ and $V(r)$ reflects the nature of the interaction, and therefore, the ratio of $G/|V|$ can be used as an appropriate index in link classification. If this ratio is less than 0.5, the nature of the interaction will be purely covalent, and if the ratio is greater than 1, the interaction may be considered as completely non-covalent. Note that for covalent bonds (i.e. $\nabla^2 \rho(r) < 0$ and $G/|V| < 0.5$), the nature of the bond from van der Waals interactions to strong covalent interactions. It becomes covalent. It can also play a decisive role in controlling the amount of ionic interaction for close-shell interactions (i.e. $\nabla^2 \rho(r) > 0$ and $G/|V| > 1$), as they become stronger ionically (and weakly electrostatic) by reducing interactions. Therefore, the QTAIM topology analysis together with WBI analysis and adsorption results expose an important trend: by increasing the ionic character of atomic bonds in the nanotubes, the tendencies of the gases to adsorb is also increased.

Considerable results can be obtained from reviewing Table 7. It is observed that in all adsorption sites Laplacian of electron

Table 7. The AIM topological parameters, including electron density ($\rho(r)$), Laplacian of electron density ($\nabla^2 \rho(r)$), the kinetic electron density $G(r)$, potential electron density $V(r)$, eigenvalues of Hessian matrix (λ) and bond ellipticity index (ϵ) at BCPs of the CFM clusters with SiCNT and SiCGeNT.

Systems	Bond	ρ	$\nabla^2 r$	$G(r)$	$V(r)$	$G(r)/V(r)$	λ_1	λ_2	λ_3	ϵ
CH ₂ ClF	C-H	0.2788	-0.9946	0.0287	-0.3061	0.0939	-0.7828	0.5499	-0.7617	0.0277
	C-Cl	0.1765	-0.1940	0.0597	-0.1680	0.3557	-0.2799	0.3517	-0.2657	0.0532
	C-F	0.2550	-0.1198	0.3286	-0.6872	0.4782	-0.4988	0.8082	-0.4292	0.1621
SiCNT	Si-C	0.1230	0.3720	0.1620	-0.231	0.7010	-0.168	0.6790	-0.139	0.2110
SiCGeNT	Si-C	0.1233	0.3721	0.1620	-0.2309	0.7014	-0.1682	0.6791	-0.1388	0.2121
	Ge-C	0.1391	0.1714	0.1250	-0.2072	0.6034	-0.1495	0.4817	-0.1607	0.0748
CH ₂ ClF/SiCNT	F-C	0.0074	0.0209	0.0043	-0.0033	1.2818	-0.0054	0.0304	-0.0041	0.3019
	F-Si	0.0193	0.0363	0.0113	-0.0135	0.8355	-0.0119	0.0599	-0.0117	0.0208
	C-H	0.2809	-1.0330	0.0268	-0.3119	0.0861	-0.7800	0.5477	-0.8007	0.0265
	C-Cl	0.1823	-0.2151	0.0614	-0.1767	0.3478	-0.2916	0.3528	-0.2764	0.0548
	C-F	0.2378	-0.1492	0.2849	-0.6072	0.4693	-0.4376	-0.3655	0.6540	0.1971
CH ₂ ClF/SiCGeNT	F-Ge	0.0243	0.0633	0.0180	-0.0203	0.8905	-0.0178	0.0997	-0.0186	0.0414
	C-H	0.2807	-1.0219	0.0276	-0.3107	0.0888	-0.7736	0.5469	-0.7953	0.0281
	C-Cl	0.1837	-0.2207	0.0619	-0.1789	0.3458	-0.2792	0.3528	-0.2943	0.0538
	C-F	0.2357	-0.1581	0.2780	-0.5955	0.4668	-0.4309	0.6325	-0.3597	0.1979

All values have been calculated using the PBE0/6-311G(d) level of theory from NBO analysis.

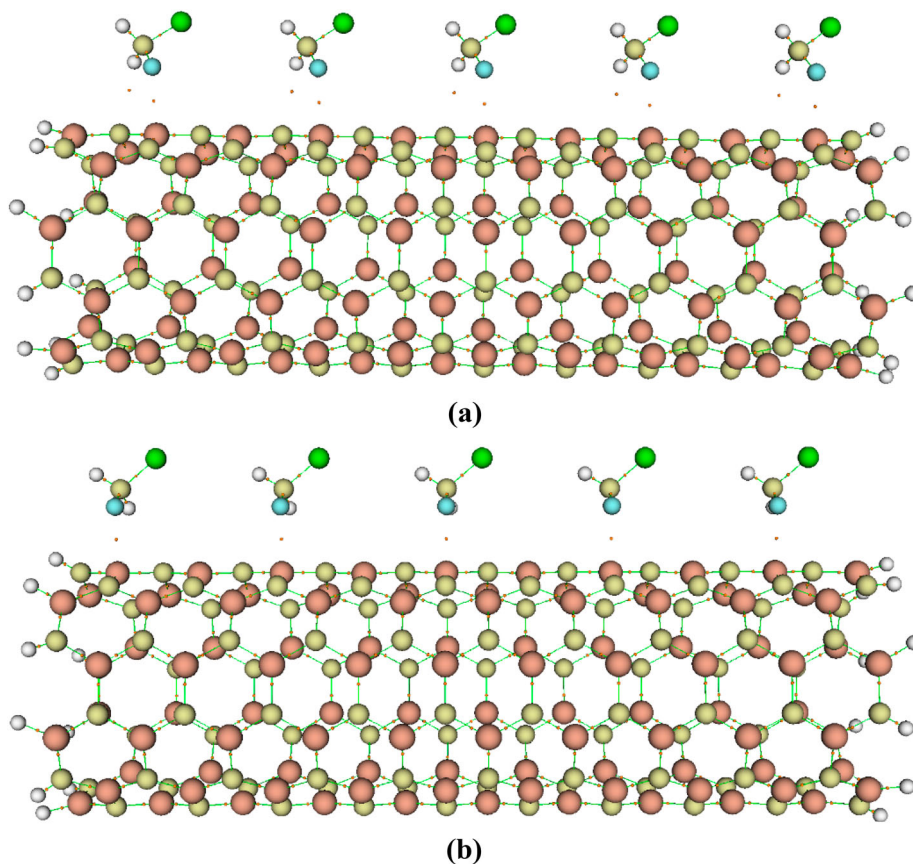


Figure 6. (Colour online) AIM molecular graphs for (a) CFM/SiCNT and (b) CFM/SiCGeNT systems. Orange dots represent the boundary critical points (BCPs).

energy density has a positive value, i.e. the bond is noncovalent. In the study of doped systems, we found that for the all clusters the energy density and the energy density of Laplacin are high indicating that there is a strong bond between the nanotubes and the CFM molecule and the elliptical bond is close to 0, which means the interaction is strong. As stated above, the ratio $G/|V|$ More than 1 means non-covalent bonding, in the case of Ge-doped clusters these amounts are less than 1. In other words, the results of QTAIM analysis also confirm the strong adsorption of the CFM molecule on the SiCGeNT which is illustrated in Figure 6.

The reduced density gradient (RDG) function as well as $\text{sign}\lambda_2(r)\rho(r)$ are used to evaluate the weak interactions. These functions are categorised in the context of non-covalent interaction methods which is powerful way to analyze the types of intermolecular interactions. The RGD is defined as follows [95, 96]:

$$\text{RDGs} = \frac{1}{2(3\pi^2)^{\frac{1}{3}}} \frac{|\overline{\Delta\rho(r)}|}{\rho(r)^{\frac{4}{3}}} \quad (24)$$

The strength of the interaction has a positive correlation with electron density $\rho(r)$ and the second largest eigenvalue of the Hessian matrix (λ_2). Thus, the real space function $\text{sign}\lambda_2(r)\rho(r)$ (the products of the signs of λ_2 and ρ) can be defined. The scatter graph of the sign of the $\lambda_2(r)\rho(r)$ function (X-axis) and RDG (Y-axis) reveals the interaction type between gases and nanotubes. The RDG values range

from medium to very large around the nuclei and edges of the molecules, whereas weak interactions (zero to medium) are observed around the chemical bonds. Also, for each specific value of RDG (seen as a horizontal line on the graph), the regions of the graph can be classified into three types, namely, $\text{sign}\lambda_2(r)\rho(r) < 0$ (strong attraction), $\text{sign}\lambda_2(r)\rho(r) \approx 0$ (weak van der Waals interaction), and $\text{sign}\lambda_2(r)\rho(r) > 0$ (strong repulsion (steric effect in ring)) [95, 96].

Using the isosurface $\text{RDG} = 0.5$ as a reference, it can be concluded that after adsorption of the gas onto the outer surfaces of the nanotubes, spots appeared around the region characterised by $\text{sign}\lambda_2(r)\rho(r) \approx 0$. The interaction of gas with SiC nanotubes are in the range of strong van der Waals interactions in nature. Significant changes in the overall features of the pristine nanotubes graph (Figure 7) after the adsorption of gases were observed in the region characterised as $\text{sign}\lambda_2(r)\rho(r) < 0$ (i.e. strong attraction), implying that the nanotube/gas interactions were strong. Hence, this analysis also confirms the results of the single-point energy calculations and NBO analysis, namely that the interactions of CFM with SiCNT and SiCGeNT were strong.

In this study, the interactions between Chlorofluoromethane molecule and pristine and Ge-doped silicon carbide nanotubes as were investigated using density functional framework. To this end, the structure of the nanotubes and CFM molecule was optimised at the theoretical level of PBE0/6-311G (d). Right after that B3LYP. CAM-B3LYP,

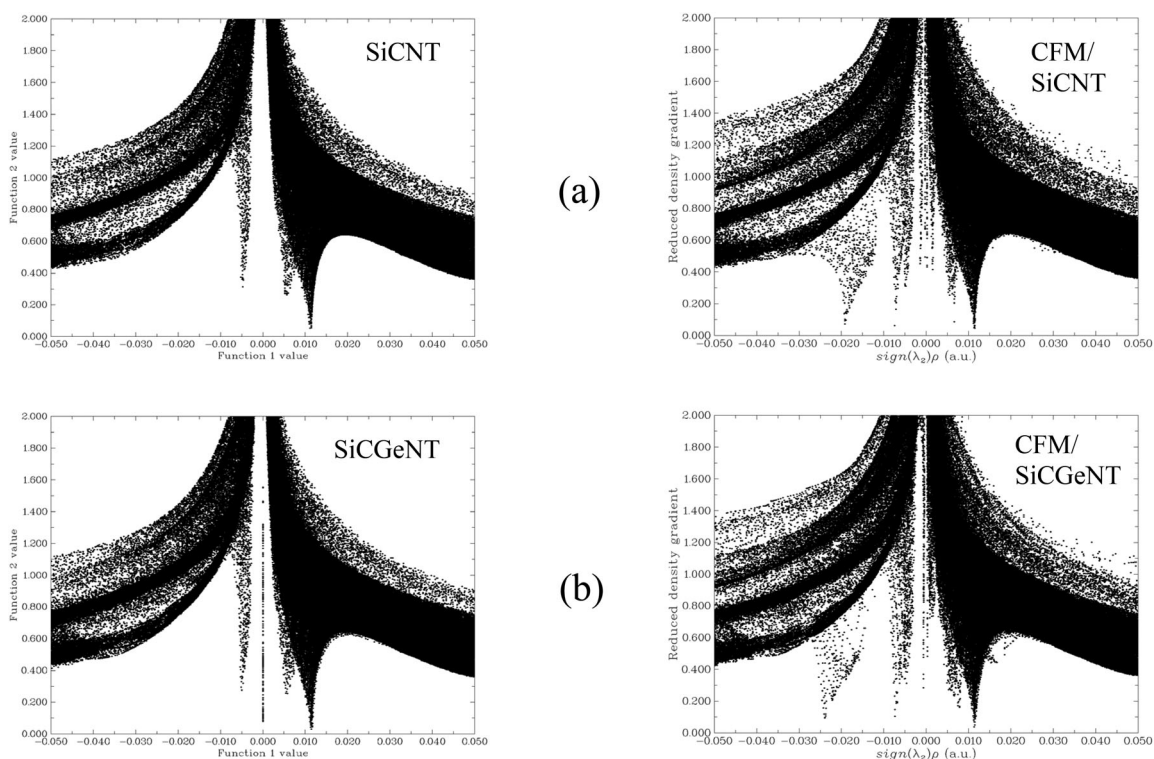


Figure 7. Plots for the reduced density gradient (RDG) vs. $\text{sign}(\lambda_2)\rho(r)$ values of the (a) pristine and (b) Ge-doped silicon carbide nanotubes. The data were obtained from completed nanotube and PBE/PBE /6-311G (d) level of theory. The left side diagrams are isolated nanotubes and the right side diagrams are CFM/nanotube clusters.

M06-2X, and ω B97XD functionals and same basis set were also used to consider the contribution of long range interactions and dispersion effect. QTAIM and NBO analyzes were also implemented to consider the character of intermolecular interactions. The results of all analyses are in agreement and show: (1) Among the different positions studied for pristine silicon carbide nanotube, the T_1 position has the highest absorption energy; (2) investigations in this study show that the Ge atom can be substituted by Si atom by chemical bonding and, as a binding element, cause dramatic changes in the chemical, electronic and mechanical structure of SiCNT nanotube; (3) the Ge-doped SiCNT has a very high adsorption energy compared to SiCNT, and is expected to be strong physical adsorption in this case and appears to be a suitable sensor characteristic option. Generally, we found that the adsorption tendencies of the aforementioned gas molecule has a positive correlation to the nature of the bonds in SiC nanotubes. Finally, we conclude that the SiCNT and SiCGeNT are favourable candidates for utilisation as gas sensor devices to detect CFM molecule.

4. Conclusion

In this study, the interactions between Chlorofluoromethane molecule and pristine and Ge-doped silicon carbide nanotubes as were investigated using density functional theory framework. To this end, the structure of the nanotubes and CFM molecule was optimised at the theoretical level of PBE0/6-311G (d). Right after that B3LYP. CAM-B3LYP,

M06-2X, and ω B97XD functionals and same basis set were also used to consider the contribution of long range interactions and dispersion effect. QTAIM and NBO analyses were also implemented to consider the character of intermolecular interactions. The results of all analyses are in agreement and show: (1) Among the different positions studied for pristine silicon carbide nanotube, the T_1 position has the highest absorption energy; (2) investigations in this study show that the Ge atom can be substituted by Si atom by chemical bonding and, as a binding element, cause dramatic changes in the chemical, electronic and mechanical structure of SiCNT nanotube; (3) the Ge-doped SiCNT has a very high adsorption energy compared to SiCNT, and is expected to be strong physical adsorption in this case and appears to be a suitable sensor characteristic option. Generally, we found that the adsorption tendencies of the aforementioned gas molecule has a positive correlation to the nature of the bonds in SiC nanotubes. Finally, we conclude that the SiCNT and SiCGeNT are favorable candidates for utilisation as gas sensor devices to detect CFM molecule.

Acknowledgements

I would like to thank the Solid-State Theory Group at the Physics Department at the Università degli Studi di Milano-Italy for providing computational facilities.

Disclosure statement

No potential conflict of interest was reported by the author(s).

References

- [1] Iijima S, Ichihashi T. Single-shell carbon nanotubes of 1-nm diameter. *Nature*. 1993;363:603–605.
- [2] Bethune D, Kiang CH, De Vries M, et al. Cobalt-catalysed growth of carbon nanotubes with single-atomic-layer walls. *Nature*. 1993;363:605–607.
- [3] Iijima S. Helical microtubules of graphitic carbon. *Nature*. 1991;354:56–58.
- [4] Mintmire JW, Dunlap BI, White CT. Are fullerene tubules metallic? *Phys Rev Lett*. 1992;68:631.
- [5] Monthieux M, Kuznetsov VL. Who should be given the credit for the discovery of carbon nanotubes? *Carbon N Y*. 2006;44:1621–1623.
- [6] Eklund P, Ajayan P, Blackmon R, et al. International assessment of research and development of carbon nanotube manufacturing and applications; 2007.
- [7] Pujadó MP. Carbon nanotubes as platforms for biosensors with electrochemical and electronic transduction. Berlin: Springer Science & Business Media; 2012.
- [8] Yu M-F, Lourie O, Dyer MJ, et al. Strength and breaking mechanism of multiwalled carbon nanotubes under tensile load. *Science*. 2000;287:637–640.
- [9] Peng B, Locascio M, Zapol P, et al. Measurements of near-ultimate strength for multiwalled carbon nanotubes and irradiation-induced crosslinking improvements. *Nat Nanotechnol*. 2008;3:626.
- [10] Filletter T, Bernal R, Li S, et al. Ultrahigh strength and stiffness in cross-linked hierarchical carbon nanotube bundles. *Adv Mater*. 2011;23:2855–2860.
- [11] Tans SJ, Devoret MH, Dai H, et al. Individual single-wall carbon nanotubes as quantum wires. *Nature*. 1997;386:474–477.
- [12] Tang Z, Zhang L, Wang N, et al. Superconductivity in 4 angstrom single-walled carbon nanotubes. *Science*. 2001;292:2462–2465.
- [13] Makarova T, Palacio F. Carbon based magnetism: an overview of the magnetism of metal free carbon-based compounds and materials. Amsterdam: Elsevier; 2006.
- [14] Zhang R, Zhang Y, Zhang Q, et al. Growth of half-meter long carbon nanotubes based on Schulz–Flory distribution. *ACS Nano*. 2013;7:6156–6161.
- [15] Medeiros PV, Marks S, Wynn JM, et al. Single-atom scale structural selectivity in Te nanowires encapsulated inside ultranarrow, single-walled carbon nanotubes. *ACS Nano*. 2017;11:6178–6185.
- [16] Berber S, Kwon Y-K, Tománek D. Unusually high thermal conductivity of carbon nanotubes. *Phys Rev Lett*. 2000;84:4613.
- [17] Pop E, Mann D, Wang Q, et al. Thermal conductance of an individual single-wall carbon nanotube above room temperature. *Nano Lett*. 2006;6:96–100.
- [18] Mingo N, Stewart DA, Broido DA, et al. Phonon transmission through defects in carbon nanotubes from first principles. *Phys Rev B*. 2008;77:033418.
- [19] Karousis N, Tagmatarchis N, Tasis D. Current progress on the chemical modification of carbon nanotubes. *Chem Rev*. 2010;110:5366–5397.
- [20] Nalwa HS. Encyclopedia of nanoscience and nanotechnology. New York: American Scientific Publishers; 2004.
- [21] Choudhary S, Qureshi S. Theoretical study on transport properties of a BN co-doped SiC nanotube. *Phys Lett A*. 2011;375:3382–3385.
- [22] Choudhary S. Spin transport in H₂O adsorbed SiCNT based magnetic tunnel junction using half metallic ferromagnetic electrodes. *Adv Sci Eng Med*. 2017;9:943–947.
- [23] Mpourmpakis G, Froudakis GE, Lithoxoos GP, et al. SiC nanotubes: a novel material for hydrogen storage. *Nano Lett*. 2006;6:1581–1583.
- [24] Wang X, Liew KM. Hydrogen storage in silicon carbide nanotubes by lithium doping. *J Phys Chem C*. 2011;115:3491–3496.
- [25] Ganji M, Ahaz B. First principles simulation of molecular oxygen adsorption on SiC nanotubes. *Commun Theor Phys*. 2010;53:742.
- [26] Cao F, Sun H. Theoretical study on the possibility of using silicon carbide nanotubes as dehydrogenation catalysts for ammonia–borane. *RSC Adv*. 2012;2:7561–7568.
- [27] Mercan K, Civalek Ö. Buckling analysis of silicon carbide nanotubes (SiCNTs). *Int J Eng Appl Sci*. 2016;8:101–108.
- [28] Mavrandonakis A, Froudakis GE, Schnell M, et al. From pure carbon to silicon-carbon nanotubes: an ab-initio study. *Nano Lett*. 2003;3:1481–1484.
- [29] Adhikari K, Ray A. Carbon-and silicon-capped silicon carbide nanotubes: an ab initio study. *Phys Lett A*. 2011;375:1817–1823.
- [30] Alam KM, Ray AK. A hybrid density functional study of zigzag SiC nanotubes. *Nanotechnology*. 2007;18:495706.
- [31] Zhang Y, Huang H. Stability of single-wall silicon carbide nanotubes—molecular dynamics simulations. *Comp Mater Sci*. 2008;43:664–669.
- [32] Baei MT, Peyghan AA, Moghimi M, et al. Effect of gallium doping on electronic and structural properties (6, 0) zigzag silicon carbide nanotube as a p-semiconductor. *J Cluster Sci*. 2012;23:1119–1132.
- [33] Mohammadi MD, Hamzehloo M. The adsorption of bromomethane onto the exterior surface of aluminum nitride, boron nitride, carbon, and silicon carbide nanotubes: a PBC-DFT, NBO, and QTAIM study. *Comp Theor Chem*. 2018;1144:26–37.
- [34] Nemat-Kande E, Abbasi M, Mohammadi MD. Feasibility of pristine and decorated AlN and SiC nanotubes in sensing of noble gases: a DFT study. *Chem Select*. 2019;4:2453–2462.
- [35] Gao K, Chen G, Wu D. A DFT study on the interaction between glycine molecules/radicals and the (8, 0) SiCNT. *Phys Chem Chem Phys*. 2014;16:17988–17997.
- [36] Javan MB. Adsorption of CO and NO molecules on SiC nanotubes and nanocages: DFT study. *Surf Sci*. 2015;635:128–142.
- [37] Gao G, Kang HS. First principles study of NO and NNO chemisorption on silicon carbide nanotubes and other nanotubes. *J Chem Theory Comput*. 2008;4:1690–1697.
- [38] Nematollahi P, Esrafil MD. A DFT study on the N₂O reduction by CO molecule over silicon carbide nanotubes and nanosheets. *RSC Adv*. 2016;6:59091–59099.
- [39] Mahdavi Z, Abbasi N, Shakerzadeh E. A comparative theoretical study of CO₂ sensing using inorganic AlN, BN and SiC single walled nanotubes. *Sens Actuat B Chem*. 2013;185:512–522.
- [40] Binbrek OS, Torrie BH, Swainson IP. Neutron powder-profile study of chlorofluoromethane. *Acta Crystallogr Sect C Crys Struct Commun*. 2002;58:o672–o674.
- [41] U.N.E.P.O. Secretariat. Handbook for the Montreal protocol on substances that deplete the ozone layer, UNEP/Earthprint; 2006.
- [42] Favero LB, Maris A, Melandri S, et al. Non covalent interactions stabilizing the chiral dimer of CH₂ ClF: a rotational study. *Phys Chem Chem Phys*. 2019;21:3695–3700.
- [43] Perdew JP, Burke K, Ernzerhof M. Generalized gradient approximation made simple. *Phys Rev Lett*. 1996;77:3865.
- [44] Hehre WJ, Ditchfield R, Pople JA. Self-consistent molecular orbital methods. XII. Further extensions of Gaussian – type basis sets for use in molecular orbital studies of organic molecules. *J Chem Phys*. 1972;56:2257–2261.
- [45] Frisch M, Trucks G, Schlegel H, et al. Gaussian 16. Wallingford: Gaussian, Inc; 2016.
- [46] Lu T, Chen F. Multiwfn: a multifunctional wavefunction analyzer. *J Comput Chem*. 2012;33:580–592.
- [47] Lu T, Chen F. Quantitative analysis of molecular surface based on improved Marching Tetrahedra algorithm. *J Mol Graph Modell*. 2012;38:314–323.
- [48] Lu T, Chen Q. A simple method of identifying π orbitals for non-planar systems and a protocol of studying π electronic structure. *Theor Chem Acc*. 2020;139:25.
- [49] Foresman J, Frisch E. Exploring chemistry with electronic structure methods: a guide to using Gaussian. Pittsburgh: Gaussian Inc.; 1996.
- [50] Parr RG, Donnelly RA, Levy M, et al. Electronegativity: the density functional viewpoint. *J Chem Phys*. 1978;68:3801–3807.
- [51] von Szentpály L. Valence states in molecules. 3. Transferable vibrational force constants from homonuclear data. *J Phys Chem A*. 1998;102:10912–10915.
- [52] Janak J. Proof that $\partial \epsilon_n / \partial n_i = \epsilon_i$ in density-functional theory. *Phys Rev B*. 1978;18:7165.

- [54] Parr RG. Density functional theory of atoms and molecules, Horizons of quantum chemistry. Berlin: Springer; 1980.
- [55] Chattaraj P, Roy D. Perennial review: update 1 of Electrophilicity Index, 2007.
- [56] Parr RG, Szentpaly LV, Liu S. Electrophilicity index. *J Am Chem Soc.* 1999;121:1922–1924.
- [57] Noorizadeh S, Maihami H. A theoretical study on the regioselectivity of Diels–Alder reactions using electrophilicity index. *J Mol Struct Theochem.* 2006;763:133–144.
- [58] Weinhold F, Landis CR. Valency and bonding: a natural bond orbital donor-acceptor perspective. Cambridge: Cambridge University Press; 2005.
- [59] Weinhold F. Discovering chemistry with natural bond orbitals. New York: John Wiley & Sons; 2012.
- [60] Carpenter J, Weinhold F. Analysis of the geometry of the hydroxymethyl radical by the “different hybrids for different spins” natural bond orbital procedure. *J Mol Struct Theochem.* 1988;169:41–62.
- [61] Foster AJ, Weinhold F. Natural hybrid orbitals. *J Am Chem Soc.* 1980;102:7211–7218.
- [62] Reed AE, Weinhold F. Natural bond orbital analysis of near-Hartree–Fock water dimer. *J Chem Phys.* 1983;78:4066–4073.
- [63] Reed AE, Weinhold F. Natural localized molecular orbitals. *J Chem Phys.* 1985;83:1736–1740.
- [64] Reed AE, Weinstock RB, Weinhold F. Natural population analysis. *J Chem Phys.* 1985;83:735–746.
- [65] Reed AE, Curtiss LA, Weinhold F. Intermolecular interactions from a natural bond orbital, donor-acceptor viewpoint. *Chem Rev.* 1988;88:899–926.
- [66] Weinhold F. Natural bond orbital methods. *Encycl Comp Chem.* New York: John Wiley & Sons; 2002.
- [67] Glendening E, Badenhoop J, Reed A, et al. Theoretical Chemistry Institute, University of Wisconsin, Madison, WI, 2001, NBO Version, 5; 2012.
- [68] Weinhold F. Natural bond orbital analysis: a critical overview of relationships to alternative bonding perspectives. *J Comput Chem.* 2012;33:2363–2379.
- [69] Glendening E, Badenhoop J, Reed A, et al. NBO 6.0, Theoretical Chemistry Institute, University of Wisconsin, Madison; 2013.
- [70] Weinhold F, Landis C, Glendening E. What is NBO analysis and how is it useful? *Int Rev Phys Chem.* 2016;35:399–440.
- [71] Glendening ED, Landis CR, Weinhold F. NBO 7.0: new vistas in localized and delocalized chemical bonding theory. *J Comput Chem.* 2019;40:2234–2241.
- [72] Mulliken RS. Electronic population analysis on LCAO–MO molecular wave functions. I. *J Chem Phys.* 1955;23:1833–1840.
- [73] Mayer I. Charge, bond order and valence in the AB initio SCF theory. *Chem Phys Lett.* 1983;97:270–274.
- [74] Mayer I. Improved definition of bond orders for correlated wave functions. *Chem Phys Lett.* 2012;544:83–86.
- [75] Giambiagi M, de Giambiagi MS, Mundim KC. Definition of a multi-center bond index. *Struct Chem.* 1990;1:423–427.
- [76] Matito E. An electronic aromaticity index for large rings. *Phys Chem Chem Phys.* 2016;18:11839–11846.
- [77] Wiberg KB. Application of the pople-santry-segal CNDO method to the cyclopropylcarbinyl and cyclobutyl cation and to bicyclobutane. *Tetrahedron.* 1968;24:1083–1096.
- [78] Mayer I, Salvador P. Overlap populations, bond orders and valences for ‘fuzzy’ atoms. *Chem Phys Lett.* 2004;383:368–375.
- [79] Lu T, Chen F. Bond order analysis based on the Laplacian of electron density in fuzzy overlap space. *J Phys Chem A.* 2013;117:3100–3108.
- [80] Sizova OV, Skripnikov LV, Sokolov AY. Symmetry decomposition of quantum chemical bond orders. *J Mol Struct Theochem.* 2008;870:1–9.
- [81] Bader R, Nguyen-Dang TT, Tal Y. A topological theory of molecular structure. *Rep Progr Phys.* 1981;44:893.
- [82] Biegler-könig FW, Bader RF, Tang TH. Calculation of the average properties of atoms in molecules. II. *J Comput Chem.* 1982;3:317–328.
- [83] Bader RF. Atoms in molecules. *Acc Chem Res.* 1985;18:9–15.
- [84] Bader RF. A quantum theory of molecular structure and its applications. *Chem Rev.* 1991;91:893–928.
- [85] Cortés-Guzmán F, Bader RF. Complementarity of QTAIM and MO theory in the study of bonding in donor–acceptor complexes. *Coord Chem Rev.* 2005;249:633–662.
- [86] Bader RF, Matta CF. Atoms in molecules as non-overlapping, bounded, space-filling open quantum systems. *Found Chem.* 2013;15:253–276.
- [87] Howard S, Krygowski T. Benzenoid hydrocarbon aromaticity in terms of charge density descriptors. *Can J Chem.* 1997;75:1174–1181.
- [88] Noorizadeh S, Shakerzadeh E. Shannon entropy as a new measure of aromaticity, Shannon aromaticity. *Phys Chem Chem Phys.* 2010;12:4742–4749.
- [89] Balanarayan P, Gadre SR. Topography of molecular scalar fields. I. Algorithm and Poincaré–Hopf relation. *J Chem Phys.* 2003;119:5037–5043.
- [90] Roy D, Balanarayan P, Gadre SR. An appraisal of Poincaré–Hopf relation and application to topography of molecular electrostatic potentials. *J Chem Phys.* 2008;129:174103.
- [91] Matta CF. Hydrogen–hydrogen bonding: the non-electrostatic limit of closed-shell interaction between two hydro, hydrogen bonding – new insights. Berlin: Springer; 2006.
- [92] Bohórquez HJ, Boyd RJ, Matta CF. Molecular model with quantum mechanical bonding information. *J Phys Chem A.* 2011;115:12991–12997.
- [93] Grabowski SJ. QTAIM characteristics of halogen bond and related interactions. *J Phys Chem A.* 2012;116:1838–1845.
- [94] Tal Y, Bader R. Studies of the energy density functional approach. I. Kinetic energy. *Int J Quantum Chem.* 1978;14:153–168.
- [95] Keith T, Bader R, Aray Y. Structural homeomorphism between the electron density and the virial field. *Int J Quantum Chem.* 1996;57:183–198.
- [96] Johnson ER, Keinan S, Mori-Sánchez P, et al. Revealing noncovalent interactions. *J Am Chem Soc.* 2010;132:6498–6506.